

8-HOQ a natural chelating agent from *Streptomyces* spp inhibits A549 lung cancer cell lines via BCL2/STAT3 regulating pathways

Joseph Devadass Balthazar (✉ drjosephdb@loyolacollege.edu)

Loyola College

Soosaimanickam Maria Packiam

Loyola College

C. Emmanuel

Gleneagles Global Health City

Krishnaraj Thirugnansambantham

Saveetha Institute of Medical and Technical Sciences

Abdullah Sheikh

King Faisal University

Saleh Fahad Alghafis

Ministry of Health

Hairul-Islam ibrahim

King Faisal University

Research Article

Keywords: Streptomyces, A549, anticancer, apoptosis, P53, STAT3, dual staining

Posted Date: June 2nd, 2022

DOI: <https://doi.org/10.21203/rs.3.rs-1709282/v1>

License: © ⓘ This work is licensed under a Creative Commons Attribution 4.0 International License.

[Read Full License](#)

Abstract

Biomolecules from *Streptomyces* spp. are emerging sources of natural drugs and have been focused on over the decade. The discovery of bioactive chemotherapeutic molecules from soil *Streptomyces* spp. has opened the medium for the search for natural drugs. In the current study, 8-HOQ was extracted and purified from soil *Streptomyces* spp and was evaluated on A549 and BEAS cell lines. The apoptotic and caspase mediated pathways were evaluated using cell proliferation, dual fluorescent staining, migration, invasion and mRNA as well as protein quantification of apoptotic markers. In vitro cytotoxicity test revealed that 8-HOQ possesses potent anticancer activities with IC₅₀ values of 26 μM, 5 μM, 7.2 μM at 24 h, 48 h, and 72 h respectively against A549 lung cancer cell lines. The result also demonstrated that 8-HOQ from *Streptomyces* spp significantly inhibited the A549 lung cancer cell lines and activated the intrinsic pathways of apoptosis. The caspase-3 and 8 activities were potentially elevated in 8-HOQ treated A549 cell lines and confirmed that 8-HOQ mediated A549 cancer cell death through the intrinsic pathway. The results explored caspase-mediated apoptosis as a mechanism underlying the inhibition of cancer cell viability in a dose-dependent manner. The expression of P53, BCL2 and STAT3 were inhibited in A549 cell lines and confirmed the metastasis inhibitory potential of 8-HOQ by blocking migration and invasion in A549 cell lines. These results indicated that 8-HOQ from *Streptomyces* spp. potentially inhibited growth and migration of A549 lung cancer cell lines.

Introduction

Bio synthesized microbial fermentation products were interestingly searched for active biomolecules from natural sources, and they pursued for an ethnobotanical approach to folk remedies for the treatment of cancer (Joseph et al., 2017). With this approach, chemical work was focused on plant species that were believed to have therapeutic effects based on local testimonials. Also, influenced by the discovery of bioactive products viz. colchicine and other bioactive compounds of plant origin. This was the foundation of antitumor drug discovery sectors on a large scale. This progress promoted antitumor drug discovery with natural products to an important area of science.

The operation of a unique mechanism of action has been observed for each of the most successful anticancer drugs. The important mechanistic category is that biomolecules interact with DNA chelating enzymes, inflammatory mediators and apoptotic markers. These are responsible for the action of many anticancer pathways. The apoptotic mediators P53 and BCL2 regulated the cancer progression and reciprocally activated the inflammatory activator STAT3 in many cancer cells (Sepúlveda et al., 2007, Islam et al., 2014, Senthil et al., 2019).

Actinomycetes were reported to produce approximately 75% of all actinobacterial secondary metabolites (Undabarrena et al., 2016). Antimicrobial and anticancer agents isolated from actinomycetes include streptomycin, rifamycin, actinomycin-D, and gentamicin, whereas anti-cancer agents comprise mitomycin, aclarubicin, doxorubicin, mithramycin, neocarzinostatin and carzinophilin (Newman et al., 2014, Njenga et al., 2017 and Olano et al., 2009).

The anthracyclines doxorubicin (adriamycin and daunomycin) (Duraipandiyan et al., 2010; Zhang et al., 2017). Adriamycin is able to induce single strand cleavages of DNA via a topo II-mediated cleavage (Dang et al., 2021). Mitomycin C is the most active antitumor antibiotic to react with two DNA nucleotides, which can result in cross-linked DNA, which are derived from various members of the *Streptomyces* genus (Song et al., 2014).

In this study, 8-HOQ was isolated (Joseph et al., 2017) and further explored its potential effect on A549 cancer cells for the novel apoptotic mediated anticancer activity.

Materials And Methods

Cell culture

Chemicals and reagents

Eagle's modified minimum essential medium (EMEM, phenol red-free), and fetal bovine serum (FBS) were obtained from Sigma Chemical Co. (St. Louis, MO). Dulbecco's minimal essential medium (DMEM) and an antibiotics solution containing 10,000 U/mL penicillin and 10 mg/mL streptomycin were obtained from Invitrogen (Carlsbad, CA). The trypsin- EDTA mixture (containing 0.25% trypsin and 0.02% EDTA) was obtained from Lonza Walkersville Walkersville, MD). P-nitrophenyl phosphate from Sigma, USA. Di nitro phenyl hydrazine from Merck, India. Caspase specific substrates 4-methyl-coumaryl-7-amide (MCA)-Leu-Glu-His-Asp-*p*-nitroaniline by caspase-9 and MCA Asp- Glu-Val-Asp-*p*-nitroaniline by caspase-3 from Merck, India. All other reagents used in this study were obtained from standard suppliers and were of analytical grade or higher. The human non-small lung cancer cell line A549 was grown in DMEM medium with L-glutamine supplemented with 10% fetal bovine serum (Gibco NY, USA) and antibiotic supplements (penicillin 100 units/ml; streptomycin 100 units/ml). The cells were maintained on this medium in 75 cm² tissue culture flasks and grown at 37°C under a humidified, 5% CO₂ atmosphere. After confluence, the cells were trypsinized and plated on 6 well and 96 well plates and were then incubated for 12 h for attachment. 8-HOQ treatment (0–24 h), depending upon the assay, the cells were lysed using 0.1% Triton X-100. The cell lysates were then used for the assay of biochemical parameters.

In-silico docking of 8-HOQ with human P53 and STAT3 mediators

The docking analysis was carried out using Auto dock tools (ADT) (Sanner, 1999) v1.5.4 and Autodock v4.2 programs. Chemical structure ligand Calcitriol was downloaded from the Pubchem database. Three dimensional structures of target protein; human p53 cancer mutant Y220C (PDB ID: 3zme) (Baud et al., 2018) and STAT3 (PDB ID: 6njs) (Bai et al., 2019) (<http://www.pdb.org>). The ligand was docked to target protein complexes with the molecule considered a rigid body and the flexible ligand. The search was extended over the whole receptor protein used as blind docking. The search was carried out with the Lamarckian Genetic Algorithm; populations of 150 individuals with a mutation rate of 0.02 were evolved for 5 generations. The results were evaluated by sorting the different complexes with respect to the predicted binding energy. A cluster analysis subsequently performed based on root mean square

deviation values, with reference to the starting geometry. The lowest energy conformation of the more populated cluster was considered the most trustable solution. Docked ligand-receptor interactions were visualized and analyzed using the Discovery Studio 2021 Client trial version.

Cell viability assay

For determining the rate of cell viability, the MTT [3-(4, 5- dimethylthiazol-2-yl)-2, 5-diphenyltetrazolium bromide] assay was used. A549 cells were seeded in 96-well plates at a density of 1×10^4 cells per well. The stock solution of 8-HOQ was diluted in 5% DMSO first and then in the culture medium immediately before addition into each well at the desired final concentrations, and the treatment usually lasted for 3 days unless noted otherwise. After each day 20 μ L MTT (at 5 mg/mL) was added to each well at a final concentration of 0.5 μ g/mL. The mixture was further incubated for 4 h, and the liquid in the wells was removed thereafter. Hundred microliters of dimethyl sulfoxide were then added to each well, incubated for 10 mins, mixed and the absorbance was read with a UV max microplate reader (biorad plate reader, USA) at 570 nm. The relative cell viability was expressed as a percentage of the control that was not treated with active fractions.

Quantification of apoptosis by Caspase-3, Caspase-8 and caspase-9

Caspase-3, Caspase-8 and caspase-9 activities in the 8-HOQ treated cells were measured in chromogenic substrate based on the amount of free *p*-nitroaniline (*p*NA) moiety released from the hydrolysis of the specific chromogenic substrate 4-methyl-coumaryl-7-amide (MCA) - Leu-Glu-His-Asp-*p*-nitroaniline by caspase-9 and MCA Asp- Glu-Val-Asp-*p*-nitroaniline by caspase-3 (Orchel et al., 2005), respectively. The optical density of free *p*NA, was proportional to the amount of caspase activity, which was measured at 405 nm.

Acridine orange staining of apoptotic cells

Acridine orange (AO) is a metachromatic dye that differentially stains the double-stranded (ds) and single-stranded (ss) nucleic acids. When AO intercalates with dsDNA it emits green fluorescence upon excitation at 480-490 nm. On the contrary, it emits red fluorescence when it interacts with ssDNA or RNA. The condensed chromatin in apoptotic cells is more sensitive to DNA denaturation than normal chromatin. Therefore, apoptotic cells display an intense red fluorescence and a reduced green emission when compared to non-apoptotic interphase cells. AO staining was done according to Senthil *et al.* (2019). Briefly, A549 cells were cultivated overnight in a 24-well microtiter plate containing the compounds to be tested 1×10^6 cells (counting was done with a hemocytometer) were washed with cold PBS and centrifuged at 4 °C and 500x g for 10 min (Remi centrifuge BL-21, India). The pellet was resuspended in 1 ml of cold PBS, to which 20 μ l of RNase A were added and incubated for 30 min at 37 °C. Prior to the addition of 200 μ l AO solution, the cell suspension was treated for 30-45 sec with 0.1 N HCl at room temperature. The cells were observed under a fluorescent microscope (Zeiss, Jena) with a green filter.

Matrigel invasion assay

A549 were incubated in DMEM-F12 with 10% FBS and collected via trypsinization. Cells (2×10^5 cells/well) in serum-free medium were added to the inner cup of a 24-well transwell chamber (Corning Life Sciences, Oneonta, NY, USA) that had been coated with 50 μ l of Matrigel (BD Biosciences, Franklin Lakes, NJ, USA; 1:10 dilution in serum-free medium). Medium supplemented with 8-HOQ to the outer cup and incubate for 24 h. After incubation, cells that had migrated through the Matrigel and the 8-mm pore size membrane were fixed, stained with hematoxylin and eosin (H&E, Sigma-Aldrich Chemical Co.), and then photographed under an inverted microscope. Each experiment was performed in triplicate.

Apoptotic gene expression by Reverse Transcriptase – PCR

Total RNA and DNA were isolated from cell lines using TRIzol (Ambion, USA) as per the manufacturer's instructions. Single strand cDNAs were synthesized from total RNA (1 μ g) using a cDNA synthesis kit (Genetech, Germany). cDNA (50 ng) were subjected to qPCR amplification using gene-specific primers (P53-FP: GCTGCTCAGATAGCGATGGTC; P53-RP: CTCCCAGGACAGGCACAAACA; Bcl2-FP: TTTCTCATGGCTGTCCTTCAGGGT; Bcl2-RP: AGGTCTGGCTTCATACCACAGGTT; NF- κ B p65-FP: ATCCCATCTTTGACAATCGTGC; NF κ B p65-RP: CTGGTCCCGTGAAATACACCTC; STAT3-FP: CAGCAGCTTGACACACGGTA; STAT3-RP: AAACACCAAAGTGGCATGTGA; beta-actin-FP: GGTCATCACCATTGGCAATGAG; beta-actin-RP: TACAGGTCTTTGCGGATGTCC). Quantitative real-time PCR (RT-qPCR) was performed with the SYBR® Select Master Mix (Applied Biosystems). The amplification protocol involved enzyme activation at 50°C for 2 min, denaturation at 95 °C for 2 min, followed by 40 cycles at 95 °C for 15 s and 60 °C for 60s. Beta actin was used as an internal control. Results were expressed as relative gene expression using 2^{(-Delta Delta C(T))} method (Livak and Schmittgen, 2001)

Immunoblot of apoptotic and cancer progressive markers

The protein lysate was prepared from 8-HOQ-treated A549 cell lines using the RIPA lysis buffer (Santa Cruz, Ca, USA). The lysates were then separated on an SDS-PAGE gel and transferred to a PVDF membrane (0.45 μ M). Western blot assays were performed with the aid of specified primary antibodies: NF κ B (mouse monoclonal antibody 1:1500) (Invitrogen, Waltham, MA, USA), STAT3 (rabbit polyclonal antibody 1:1000) (Invitrogen, Waltham, MA, USA), P53 (rabbit polyclonal antibody 1:1000) (Biorbyt, Cambridge, UK), COX2 (rabbit polyclonal antibody 1:1000) (Biorbyt, Cambridge, UK), β -actin (rabbit polyclonal antibody 1:2000) (Cell Signaling Technology, Beverly, MA, USA). All the antibodies were coated with HRP-labeled secondary antibodies (Khalil et al., 2022), followed by detection with an enhanced chemiluminescence reagent. Chemiluminescence of expressed bands was examined to confirm the linear range of the signals, and the quantifications were performed using the densitometry tool in ImageJ software v1.8.

Statistical analyses

The experimental data were analyzed by One-way Analysis of Variance (ANOVA) to determine the significance of different treatments at $p < 0.05$ level. All statistical analyses were carried out using the SPSS statistical package (SPSS, Version 10.0 for Windows, SPSS, Chicago, USA).

Results

***In-silico* binding of 8-HOQ on apoptotic and angiogenic marker**

In silico evaluation of apoptogenic marker mutated P53 and angiogenic marker STAT3 were studied using auto dock docking tools. The 8-HOQ acts as ligand for mutated human P53 and STAT3 protein receptors. The ligand 8-HOQ bound with P53 at the active site pocket, it is competitive to substrate binding at a site. Figure 1A,1B showed docking details between 8-HOQ with P53 and found three and four hydrogen bonds docked with short Armstrong length (Table 2) respectively. These results revealed that the bond was covalently formed with binding energy -5.4 against arginine and cysteine amino acid residues (Fig. 1B).

Cell viability and Cytotoxicity test

Cytotoxicity assay on A549 and BEAS cell lines using 8-HOQ, showed considerable toxicity on lung cancer cells than in BEAS cell lines. 8-HOQ showed a dose and time dependent Cytotoxicity in the A549 lung cancer cell line (Figure-2A). The IC₅₀ values of 8-HOQ for the three incubation duration were noticed to be 26 μ M, 5 μ M, 7.2 μ M at 24 h, 48 h, and 72 h respectively against A549 lung cancer cell lines. Whereas, 8-HOQ was least toxic to the BEAS cell line at the above concentrations and incubation durations. At 50 and 100 μ M/well concentration showed 23% of cell death at 72h of drug concentration against BEAS cell lines (Figure 2B). In conclusion, 8-HOQ was cytotoxic to normal cell lines only at higher concentrations. Fifty percent of cytotoxicity reached at 12 μ g/ml for A549 and 350 μ g/ml for BEAS normal lung cell lines and these values were considered as IC₅₀ for the respective cells correspondingly.

Acridine orange staining for apoptotic evaluation.

The potency of 8-HOQ to induce apoptosis in A549 cells was analyzed using AO/EB dual staining. Staining of cells with AO/EB stain clearly indicated 8-HOQ mediated apoptosis due to nuclear damage and accumulation of the lysozymes around the apoptotic bodies in a dose dependent manner (Fig. 3A-C) showed 8-HOQ treated cells, which depict the transition of double-stranded DNA to single-stranded DNA.

Effect of 8-HOQ on invasive capacity of A549 cell.

The effect of 8-HOQ on the invasion of A549 cells was investigated *in-vitro* by using a Boyden chamber Transwell assay and cell migration assays. A549 cells were inoculated with 8-HOQ in twelve well inserts and incubated for 4 h. The effect of 8-HOQ ties up the invasion and controls the migratory A549 cells in the gelatin matrigel membrane. (Figures 4A,4B). The invasion was significantly inhibited at 10 μ M compared to 5 μ M concentration ($p \leq 0.01$). Moreover, the angiogenic capacity was significantly high, at

about 0.29 fold in untreated A549 cancer cell lines (Figures 4). These results clearly demonstrated anti-angiogenic potential of the 8-HOQ.

Caspase quantification for activation of apoptosis.

To confirm caspase-3 activity, the 8-HOQ was treated against A549 cells, a colorimetric assay was performed to measure the increase in caspase-3 activity level (Fig. 4). In comparison to the control cells, 8-HOQ treatments increased 3 fold ($p < 0.05$). Higher caspase-3 activity could cleave cytoskeletal proteins leading to apoptosis. Caspase-8 activity was assessed similarly to the previous treatment pattern (Fig. 4). Compared to the control, treatments with 8-HOQ caused an increase in caspase-8 activity ($p < 0.02$). Similarly, treatments with 8-HOQ showed a significant difference in caspase-9 activity ($p < 0.04$) and ($p < 0.03$), compared to the control cells. These results indicated that 8-HOQ mediated caspase-8 and caspase-9 activation could consecutively activate the executioner caspase-3 for apoptosis in A549 lung cancer cells.

Gene expression analysis of apoptotic and angiogenic marker

The apoptotic genes and anti-apoptotic genes were evaluated by the mRNA expression pattern. The expression of P53 mRNA was up-regulated in all the tested conditions. Treatment with 5 and 10 μM of 8-HOQ showed 2.9 and 5.2 fold up regulation of P53 mRNA in comparison with control cells. Whereas, the expression of BCL-2 mRNA was downregulated at higher concentrations (10 μM). A similar pattern of protein expression was noticed for both P53 and BCL2 in response to 8-HOQ treatments on A549 lung cancer cell lines (Figure 5 A-C).

The angiogenic and cancer progressive marker NF κ B and STAT3 were quantified in 8-HOQ-treated A549 cell lines. Although the expression of NF κ B mRNA was unaffected at lower study concentration (5 μM), its expression was downregulated significantly by 8-HOQ treatment at higher concentrations (10 μM). The results also demonstrated that 8-HOQ treatment reduced the phosphorylation of p65-NF κ B. Whereas, in the case of STAT3, 8-HOQ treatment inhibited both mRNA expression of p-38 phosphorylation of the STAT3 protein in dose dependent manner. The treated cells revealed the extra nuclear localization of NF κ B and regulated the proteolytic phosphorylation of NF κ B transport in the nuclear membrane (Figure 6A-C). Thus, the results clearly demonstrated that 8-HOQ treatment decreased phosphorylation of both NF κ B and STAT3, which subsequently attenuated their translocation to the nucleus, its DNA-binding, and down regulated the target gene expression (Figure 6).

Discussion

Due to the variety of bioactive molecules produced, the actinomycetes are considered to be significant anticancer agents. There is a lot of research going on natural products as anticancer agents from bacteria such as streptomycetes (Shabaan et al., 2012). In this study, the 8-HOQ extracted from *Streptomyces rochei* (ERI-15) (Joseph et al., 2017) showed 79% cell inhibition of A549 lung cancer cell lines and IC₅₀ of cancer cell lines is comparatively less toxic on normal BEAS cell lines. Similarly, the

crude extract of streptomycetes strain MUM256 showed varying levels of inhibition in A549 lung cancer cell lines at higher concentrations and 8-HOQ was less toxic to the normal cell line (Tan et al., 2015). 8-HOQ is a strong bioactive compound with antibacterial and antifungal activities. It is used in agriculture to kill fungi due to the copper chelating property (You et al., 1999). Different microorganisms were reported with 8-HOQ and its derivatives such as *Streptomyces griseoflavus*, *Pseudomonas* sp., *Comamonas* sp., for 3-HOQ-2-carboxylic acid, 4-HOQ, 2-HOQ respectively (Mack and Zeeck 1987; Hwang et al., 1998; Suganya et al., 2005). Moreover, *B. subtilis*, *E.coli*, *Trichophyton rubrum* were susceptible to polymers having 8-HOQ (Kenawy 2001).

Streptomyces produce secondary metabolites such as carotenoids, flavonoids, phenols and tocopherols which have bioactive roles (Allemailem 2021; Wei et al., 2017). Moreover, they have antibacterial, antioxidant, anti-inflammatory, antiprotozoal, cytotoxic and anti-tumor properties (Almuhayawi et al., 2021, Ayswaria et al., 2020). There are numerous phenolic compounds extracted from *actinomycetes* that have anti-tumor properties (Newman & Cragg 2007; Olano et al., 2009). From this study, in agreement with the previous studies, the streptomycetes showed anticancer activity against various cancer cell lines including A549, Caco-2, HeLa, PC-3, THP and others (Graf et al., 2007; Rather et al., 2014; Kumar et al., 2021). One of the studies reported cytotoxic effects of *Streptomyces lavendulae* against A549 lung cancer cell growth (Kumar et al., 2021). In this current study, 8-HOQ from *Streptomyces* alleviates the A549 migration and invasion and induces apoptosis by down regulating the BCL2 anti-apoptotic protein (Figure 6a-c).

Angiogenesis is the key process in tumor formation, invasion and metastasis as it provides nourishment (Carmeliet and Baes 2008). So, it could be the potential antitumor approach to inhibit angiogenesis. In this study the angiogenic markers NFkB and STAT3 were inhibited in A549 cancer cells with the 8-HOQ treated cancer cells significantly (Figure 4). Similarly results observed that, 8-HOQ was interacted with antiproteosome and anti-angiogenesis process (Yang et al., 2014). Furthermore studies, 8-HOQ along with the ruthenium complex showed anti-angiogenesis and antitumor activity by inhibiting the bFGF cytokines (Yang et al., 2014)

Streptomyces scabrisporus showed antitumor activity in the cancer cell lines A549, HCT-116, HL-60, MCF-7, MDA-MB-231, MiaPaca-2, N2a, and PC-3 (Shah et al., 2016). Among the extracted metabolites 8-HOQ was observed with higher antibacterial and antifungal properties (Kolla et al., 2008). Hydroxyquinoline mediated caspase-9 activity and down regulated the caspase -3 activity in the current study and similarly, a compound from the streptomycetes (quercetin 3-O-β-L-rhamno pyranosyl-(1→6)-β-D- glucopyranoside) exhibited the cytotoxicity in A549 lung cancer cell lines by augmenting caspase-3 and caspase-9 pathways and inhibiting the BCL2 protein synthesis (Islam et al., 2014). Likewise, in leukemia, it was observed that metabolites from *Streptomyces lavis* progressed apoptosis by enhancing caspase-3 and inhibiting BCL2 (Valipour et al., 2018).

Conclusion

In the present study the purified compound 8-HOQ, from soil *Streptomyces* spp. studied for cytotoxic effect on A549 cancer cell lines, which revealed that it has potentially inhibited the A549 cancerous cells through caspase-3, and caspase-8 apoptotic mediated pathways. Additionally, the P53, BCL2 and STAT3 were down regulated through blocking of migration and invasion.

References

1. Allemailem KS. Antimicrobial Potential of Naturally Occurring Bioactive Secondary Metabolites. J Pharm Bioallied Sci. 2021 Apr-Jun;13(2):155-162.
2. Almuhayawi, M.S.; Mohamed, M.S.M.; Abdel-Mawgoud, M.; Selim, S.; Al Jaouni, S.K.; AbdElgawad, H. Bioactive Potential of Several Actinobacteria Isolated from Microbiologically Barely Explored Desert Habitat, Saudi Arabia. Biology 2021, 10, 235. <https://doi.org/10.3390/biology10030235>
3. Ayswaria R, Vasu V, Krishna R. Diverse endophytic *Streptomyces* species with dynamic metabolites and their meritorious applications: a critical review. Crit Rev Microbiol. 2020 Nov;46(6):750-758.
4. Bai L, Zhou H, Xu R, Zhao Y, Chinnaswamy K, McEachern D, Chen J, Yang CY, Liu Z, Wang M, Liu L, Jiang H, Wen B, Kumar P, Meagher JL, Sun D, Stuckey JA, Wang S. A Potent and Selective Small-Molecule Degradator of STAT3 Achieves Complete Tumor Regression In Vivo. Cancer Cell. 2019;36(5):498-511.e17.
5. Baud MGJ, Bauer MR, Verduci L, Dingler FA, Patel KJ, Horil Roy D, Joerger AC, Fersht AR. Aminobenzothiazole derivatives stabilize the thermos labile p53 cancer mutant Y220C and show anticancer activity in p53-Y220C cell lines. Eur J Med Chem. 2018. 152:101-114.
6. Carmeliet P, Baes, N. Metabolism and Therapeutic Angiogenesis Engl. J. Med., 2008, 358, 2511–2512.
7. Dang YF, Yang SH, Jiang XN, Gong FL, Yang XX, Cheng YN, Guo XL. (2021). Combination treatment strategies with a focus on rosiglitazone and adriamycin for insulin resistant liver cancer. J Drug Target.29(3):336-348.
8. Graf E, Schneider K, Nicholson G, Ströbele M, Jones AL, Goodfellow M, Beil W, DS R, Fiedler HP. 2007. Elloxazinones A and B, new aminophenoxazinones from *Streptomyces griseus* Acta 2871. J. Antibiot, 60, 277–284.
9. Hwang S.Y., S.H. Lee, K.J. Song, Y.P. Kim and K. Kawahara. 1998. Purification and characterization of antistaphylococcal sub-stance from *Pseudomonas* sp.KUH-001. J. Microbiol. Biotechnol. 8: 111–118.
10. Islam VI, Saravanan S, Ignacimuthu S. Microbicidal and anti-inflammatory effects of *Actinomadura spadix* (EHA-2) active metabolites from Himalayan soils, India. World J Microbiol Biotechnol. 2014; 30(1):9-18.
11. Joseph DB, Paulraj MG, Ignacimuthu S, et al. 2016. Antimicrobial activity of soil actinomycetes isolated from Western Ghats in Tamil Nadu, India. J Bacteriol Mycol.3(2):224-232.

12. Kenawy E. 2001. Biologically active polymers. IV. Synthesis and antimicrobial activity of polymers containing 8-HOQ moiety. *J. Appl. Polymer Sci.* 82: 1364–1374.
13. Kumar P, Chauhan A, Kumar M, Kuanr BK, Kundu A, Solanki R, Kapur MK. In vitro and in silico anticancer potential analysis of *Streptomyces* sp. extract against human lung cancer cell line, A549. *3 Biotech.* 2021 Jun;11(6):254.
14. Livak KJ and Schmittgen TD (2001). Analysis of relative gene expression data using real-time quantitative PCR and the 2(-Delta Delta C(T)) Method. *Methods*, 25, 402–408.
15. Mack S.B. and A. Zeeck. 1987. Secondary metabolites by chemical screening I. Calcium 3-hydroxyquinoline-2-carboxylate from a *Streptomyces*. *J. Antibiot.* 40: 953–960.
16. Narayana, Kolla JP, et al. "Study on bioactive compounds from *Streptomyces* sp. ANU 6277." *Polish Journal of Microbiology* 57.1 (2008): 35.
17. Newman DJ, Cragg GM. 2016 Natural products as sources of new drugs from 1981 to 2014. *J. Nat. Prod.* 79, 629–661. (doi:10.1021/acs.jnatprod.5b01055).
18. Njenga WP, Mwaura FB, Wagacha JM, Gathuru EM. 2017 Methods of isolating actinomycetes from the soils of Menengai Crater in Kenya. *Arch. Clin. Microbiol.* 8, 3. (doi:10.4172/1989-8436.100045)
19. Olano, C.; Méndez, C.; Salas, J.A. Antitumor compounds from actinomycetes: From gene clusters to new derivatives by combinatorial biosynthesis. *Nat. Prod. Rep.* 2009, 26, 628–660.
20. Orchel A, Dzierzewicz Z, Parfiniewicz B, Weglarz L, Wilczok T. 2005. Butyrate induced differentiation of colon cancer cells is PKC and JNK dependent. *Dig Dis Sci* 50: 490–498.
21. Rather, S.A.; Kumar, S.; Rah, B.; Arif, M.; Ali, A.; Qazi, P. A potent cytotoxic metabolite from terrestrial actinomycete, *Streptomyces collinus*. *Med. Chem. Res.* 2014, 23, 382–387.
22. Sanner MF. Python: a programming language for software integration and development. *J Mol Graph Model.* 1999 (1):57-61. PMID: 10660911.
23. Senthil KV, Kumaresan S, Tamizh MM, Hairul-Islam MI, Thirugnanasambantham K. Anticancer potential of NF- κ B targeting apoptotic molecule "flavipin" isolated from endophytic *Chaetomium globosum*. *Phytomedicine.* 2019 Aug;61:152830.
24. Sepúlveda, P., Encabo, A., Carbonell-Uberos, F. *et al.* BCL-2 expression is mainly regulated by JAK/STAT3 pathway in human CD34⁺ hematopoietic cells. *Cell Death Differ* **14**, 378–380 (2007). <https://doi.org/10.1038/sj.cdd.4402007>.
25. Shah, A.M.; Wani, A.; Qazi, P.H.; Rehman, S.; Mushtaq, S.; Ali, S.A.; Hussain, A.; Shah, A.; Qazi, A.K.; Makhdoomi, U.S. Isolation and characterization of alborixin from *Streptomyces scabrisporus*: A potent cytotoxic agent against human colon (HCT-116) cancer cells. *Chem. Biol. Interact.* 2016, 256, 198–208.
26. Song X, Dilly AK, Kim SY, Choudry HA, Lee YJ. Rapamycin-enhanced mitomycin C-induced apoptotic death is mediated through the S6K1-Bad-Bak pathway in peritoneal carcinomatosis. *Cell Death Dis.* 2014 Jun 5;5(6):e1281.

27. Undabarrena A, Beltrametti F, Claverías FP, González M, Moore ERB, Seeger M, Cámara B. 2016 Exploring the diversity and antimicrobial potential of marine actinobacteria from the Comau Fjord in Northern Patagonia, Chile. *Front. Microbiol.* 7, 1–16. (doi:10.3389/fmicb.2016. 01135)
28. Duraipandiyar V, Sasi A.H., Islam V.I.H., Valanarasu M., Ignacimuthu S. (2010). Antimicrobial properties of actinomycetes from the soil of Himalaya. *Journal de Mycologie Médicale.* 20, (1) 15-20.
29. Valipour, B.; Mohammadi, S.M.; Abedelahi, A.; Maragheh, B.F.A.; Naderali, E.; Dehnad, A.; Charoudeh, H.N. Culture filtrate ether extracted metabolites from *Streptomyces levis* ABRINW111 increased apoptosis and reduced proliferation in acute lymphoblastic leukemia. *Biomed. Pharm.* 2018, 108, 216–223.
- Patterson, J.T. 1987. *The Dread Disease: Cancer and Modern American Culture.* Harvard University Press: Cambridge, MA.
30. Wei, Z.; Xu, C.; Wang, J.; Lu, F.; Bie, X.; Lu, Z. Identification and characterization of *Streptomyces flavogriseus* NJ-4 as a novel producer of actinomycin D and holomycin. *PeerJ* 2017, 5, e3601.
31. Yang, Licong, et al. "Interaction between 8-hydroxyquinoline ruthenium (II) complexes and basic fibroblast growth factors (bFGF): inhibiting angiogenesis and tumor growth through ERK and AKT signaling pathways." *Metallomics* 6.3 (2014): 518-531.
32. You B.Y., Y.H. Wang and M.L. Kuo. 1999. Evaluation of geno- toxicity and carcinogenicity on fungicide, copper 8-hydroxyquino- linatate, by short-term tests. *Zhiwu Baohu Xuehui Huikan* (in Chinese) 41: 119–130.
33. Zhang XG, Liu ZY, Liu JW, Zeng YL, Guo GJ, Sun QY. (2017) Antitumor activity of a *Rhodococcus* sp. Lut0910 isolated from polluted soil. *Tumour Biol*; 39(6):1010428317711661.

Tables

Tables 2 is not available with this version.

Figures



Figure 1

In silico docking of 8-HOQ (CID: 1923) and human p53 cancer mutant Y220C (PDB ID: 3zme) and STAT3 (PDB ID: 6njs) proteins binding analysis. (A,B) Computational binding was performed using AutoDock software to demonstrate the interactions of the hydrophobic bond and other polar bonds of P53 and STAT-3. It shows the amino acid residue analysis of the interacted bond and its length, together with the binding pocket of ligand–receptor interactions.

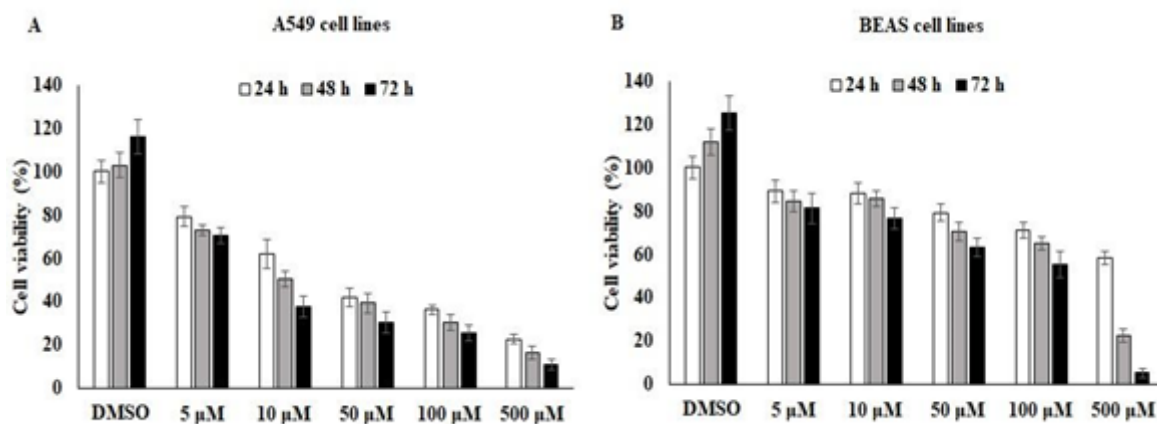


Figure 2

Effect of 8-HOQ on A549 lung cancer cell lines and BEAS normal lung cell lines. These cells were cultured in adherent-coated 48-well plates. Cultured cells were treated with 8-HOQ for three different intervals (24h, 48 h, 72h). Treated cells were evaluated for cell proliferation using SRB cytotoxicity assay. Values are expressed as three independent experiments and all values are expressed as mean \pm SD.



Figure 3

Analysis of 8-HOQ induced apoptosis in A549 lung cancer cells using Acridine Orange/Ethidium Bromide dual staining. A. Phase contrast image of control and 8-HOQ treated A549 cells under 10X observation lens. B. Fluorescence image of control and 8-HOQ treated/dual stained A549 cells showing apoptosis. C. Level of 8-HOQ induced apoptosis as measured by the intensity of apoptotic fluorescence. Values represent the mean \pm SD of triple experiments. * $P > 0.05$, compared with the DMSO group.

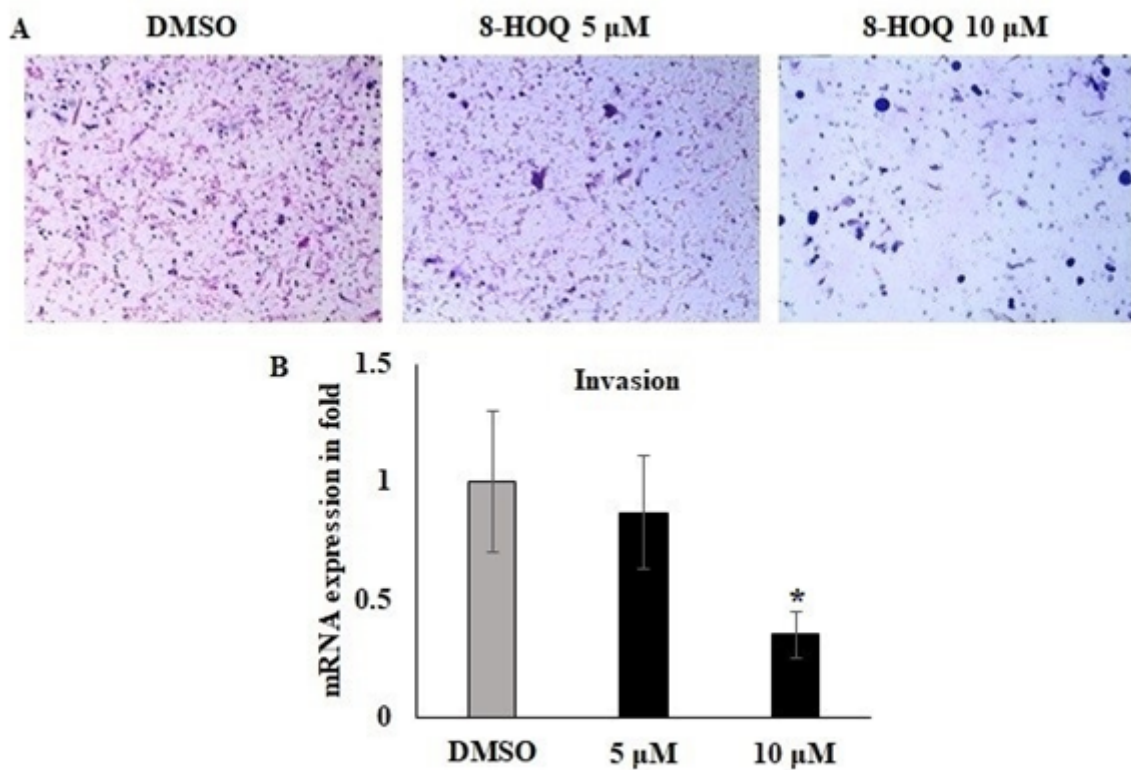


Figure 4

Effect of 8-HOQ on A549 lung cancer cell lines. 5×10^4 cells were seeded in an adherent-coated 24-well plate. 8-HOQ mitigates the invasion of A549 cells. Invasiveness of cancer cells was studied using the Boyden chamber insert well model. A549 invading capacity using gelatin coated insert well method. The invaded cells were stained with Giemsa and counted in 4 different microscopic fields. Values represent the mean \pm SD of triple experiments. * $P > 0.05$, compared with the DMSO group.

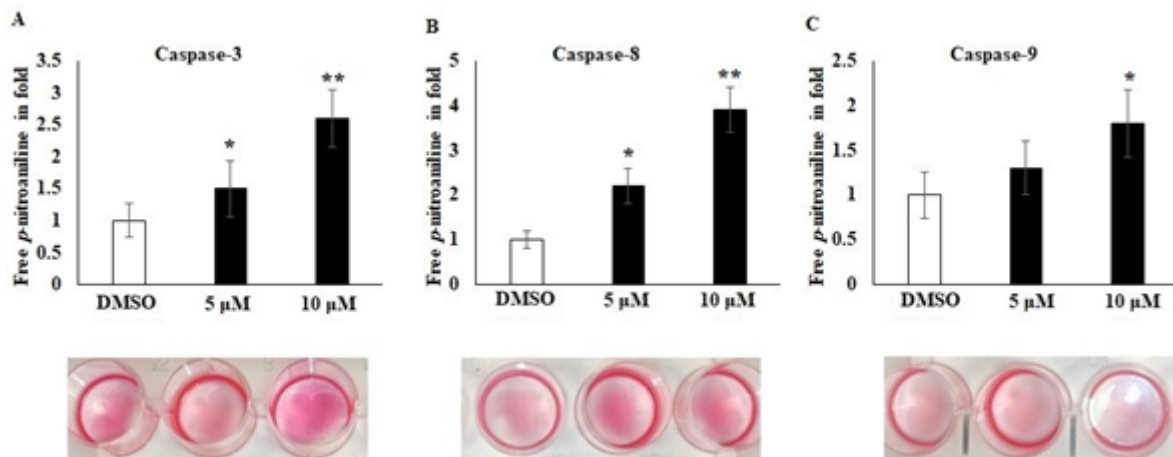


Figure 5

Effect of 8-HOQ on intrinsic and extrinsic apoptotic marker of A549 lung cancer cell lines. A-C: Caspase-3, 8 and 9 were quantified using substrate based cleavage ELISA assay in 8-HOQ treated A549 lung cancer cell lines. Alterations in the caspase expression were also denoted in the tested 48 wells culture plate and inspected using release of para nitroaniline -pNA (pink color). The experimental data are shown as mean \pm SD of triplicate values; * significant difference between untreated groups Vs. 8-HOQ treated groups. * indicates the significance $p < 0.05$ and ** indicates the significance $p < 0.001$

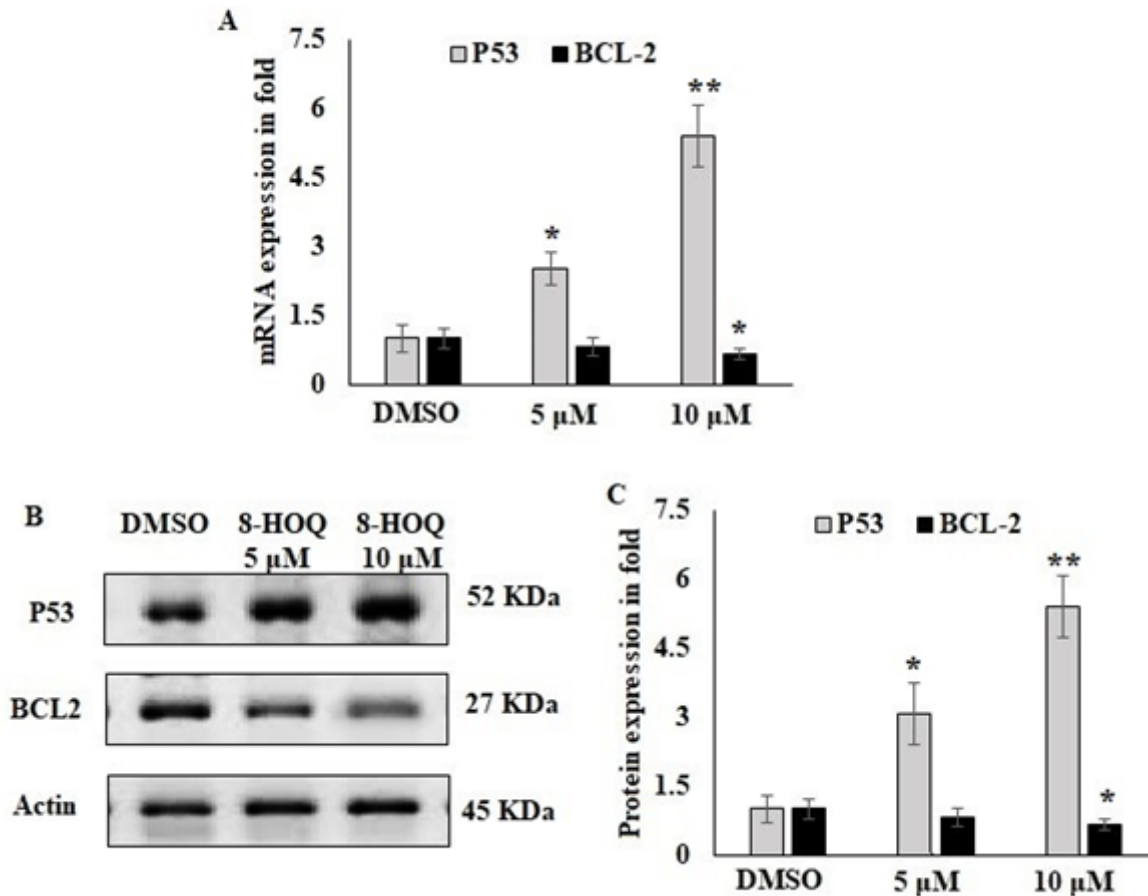


Figure 6

Effects of 8-HOQ on mRNA and protein expression of P53 and BCL2 markers of A549 lung cancer cell lines. A. 8-HOQ reciprocally regulates mRNA of P53 and BCL2 markers. B and C. Alterations in the status of protein expression in response to 8-HOQ on immuno blot. β -Actin was utilized as a control. The experimental data are shown as mean \pm SD of triplicate values; * significant difference between untreated groups Vs 8-HOQ treated groups. * indicates the significance $p < 0.05$ and ** indicates the significance $p < 0.001$

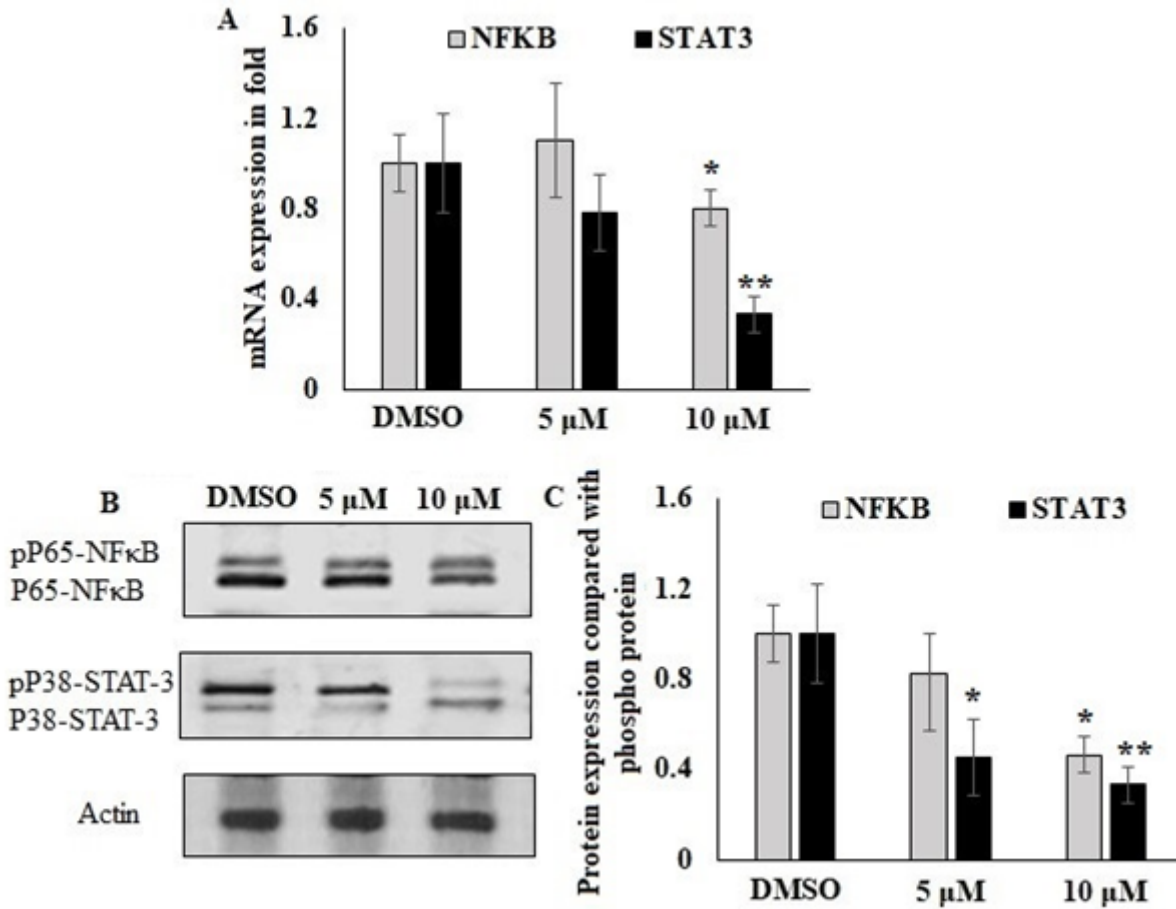


Figure 7

Effects of 8-HOQ on mRNA and protein expression of NFκB and STAT-3 angiogenic markers of A549 lung cancer cell lines. A. 8-HOQ reciprocally abrogates mRNA of NFκB and STAT-3 markers. B and C. Alterations in the status of protein expression of NFκB and STAT-3 in response to 8-HOQ using immuno blot. β-Actin was utilized as a control. The experimental data are shown as mean ± SD of triplicate values; * significant difference between untreated groups Vs 8-HOQ treated groups. * indicates the significance $p < 0.05$ and ** indicates the significance $p < 0.001$

Supplementary Files

This is a list of supplementary files associated with this preprint. Click to download.

- [S1.jpg](#)
- [S2.jpg](#)
- [S3.jpg](#)
- [S4.jpg](#)
- [S5.jpg](#)

- S6.jpg
- S7.jpg